Application Note: 50811

Nondestructive Thickness Determination of Coatings and Layers from Sub-micron to Tens of Microns Using Step-Scan FT-IR Photoacoustic Phase Spectroscopy

Key Words

- Coatings & Layers
- Depth Profiling
- Food Packaging
- Nondestructive Thickness Measurements
- Phase Modulation
- Photoacoustic Spectroscopy
- Step-Scan FT-IR

Abstract: This work examines a simplified phase difference model for the thickness measurement of organic coatings and laminates using photoacoustic spectroscopy. Step-scan phase-modulation FT-IR photoacoustic spectroscopy ($S^2\Phi M$ PAS) is utilized. This technique is highly effective for measuring thicknesses of layers from tens of microns to tenths of a micron, even for optically challenging samples.

Introduction

Coated and layered materials are common in many commercial applications and the ability to spectroscopically characterize these laminate systems is invaluable to the researcher or engineer. IR microspectroscopy can discretely analyze regions as small as 10 µm, however, this method normally requires intensive and destructive sample preparation such as thin-sectioning. Variable angle ATR analysis is nondestructive but offers only a limited probing range.[1, 2] Confocal Raman microspectroscopy has appeared as a viable technique for nondestructive depth profiling, but this technique is highly dependent on the optical properties of the sample, and in the best cases is limited to a depth resolution of approximately 2 µm.[3] FT-IR photoacoustic spectroscopy (PAS) offers both nondestructive depth analysis and the ability to work with optically challenging samples.[4, 5,6] The step-scan phase modulation ($S_2\Phi M$) PAS experiment greatly simplifies the interpretation of the probing depth. Additionally, with an appropriate phase difference model, this technique can determine layer thickness on the order of 0.1 µm.

Theory of FT-IR Photoacoustic Spectral Depth Profiling

In the PAS experiment, probing depth is identified with the thermal diffusion length which is described by [4]

$$\mu = (\alpha/\pi f)^{1/2} \quad (1)$$

In $S^2\Phi M$ PAS, f is the phase modulation frequency and the probing depth is constant across the spectrum. During data collection, the DSP processor on the Nicolet™ 8700 demodulates the signal from the PA detector to simultaneously extract the in-phase (I) and quadrature (Q) interferogram components, relative to the modulation phase. In essence, the I component is the "surface" signal, and the Q component contains the "deeper" information, delayed as the thermal wave propagates through the sample, when the surface reference phase is set properly. The magnitude PA spectrum (M) is calculated from the root mean square of the I and Q components: $M = (I^2 + Q^2)^{1/2}$. Within the probing range, deeper signals will reach the detector at larger phase lags. Phase rotation allows maximizing PA signals from different depths at certain phase angles (θ) using the following algorithm:

$$S(\theta) = I \cos\theta + Q \sin\theta \quad (2)$$

The maximum of a plot S(θ) vs. θ for a particular wavelength indicates the relative phase position at which the particular band reaches the maximum. Alternatively, this same information can be obtained from a phase spectrum (Φ) which is calculated from:

$$\Phi = \tan^{-1}(Q/I) \quad (3)$$

We presented a series of models relating the phase difference between PA signals from different layers of a polymer laminate for incorporating the optical and thermal properties of the material to the limits of the basic theory.[7] In the limiting case of optically/thermally thick layers, the expression is:

$$\Delta\Phi_{kj} = \sum_{n=j}^{k-1}\left(\frac{d_n}{\mu_n}\right) + \tan^{-1}\left[\frac{\beta_j\mu_j - \beta_k\mu_k}{1 + (\beta_j\mu_j + 1)(\beta_k\mu_k + 1)}\right] \quad (4)$$

where the optical absorption coefficient, β = abs./thickness. However, if the strongest band from each layer is used to calculate the phase difference , then β_j and β_k become large and the right hand term becomes ≈ 0. Therefore, the simplified model reduces to:

$$\Delta\Phi_{kj} = \sum_{n=j}^{k-1}\left(\frac{d_n}{\mu_n}\right) \quad \text{or} \quad d_j = \mu_j(\Delta\Phi_{kj}) \quad (5)$$

which is much more convenient for experimental layer thickness determination.

Methods and Instrumentation

$S^2\Phi M$ PAS spectra were measured using a Thermo Scientific Nicolet 8700 FT-IR spectrometer and an MTEC 300 photoacoustic accessory. The spectrometer was fitted with a Ge-on-KBr beamspltter and an air-cooled IR source. The bench was purged with dry, CO_2-free air, and the cell was purged with high-purity He. A 1975 cm^{-1} long-wave-pass filter was placed in the beam before the PA cell to optically limit the spectral range and increase the efficiency of the step-scan collect. Phase referencing was performed using a glassy carbon reference. Instrument control, data collection, and analysis were performed using the Thermo Scientific OMNIC™ software package.

Thermo SCIENTIFIC

Results and Discussion

1. Food Packaging Laminate

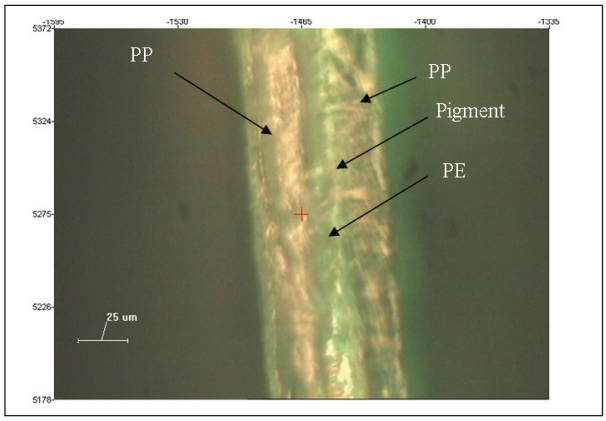

Figure 1: Micrograph of food packaging laminate showing 4 discrete layers (*l. to r.*- polypropylene, polyethylene, light green pigment layer, polypropylene)

The first sample in this study is a commercial food packaging laminate made up of four layers shown in the micrograph in Figure 1. The polymer layers in this sample are relatively thick making it a good sample to test the effectiveness of the simplified model. Figure 2 contains the $S^2\Phi M$ PAS magnitude spectra of the sample at ΦM frequencies ranging from 300 to 100 Hz. As the modulation frequency decreases, one can clearly see the appearance of bands from underlying layers begin to appear. Reference spectra indicated that the 1382 and the 1732 cm^{-1} bands were the strongest bands from the polypropylene and pigment layers, respectively. Figure 3 shows an example of a plot of the S(θ) vs. θ depicting the phase difference between the signals from these two layers.

Replicate $S^2\Phi M$ PAS data sets were collected at each of the four modulation frequencies and the phase maximum for the polypropylene and pigment bands was determined. These results are tabulated in Table 1 along with the thickness calculation for the polypropylene layer.

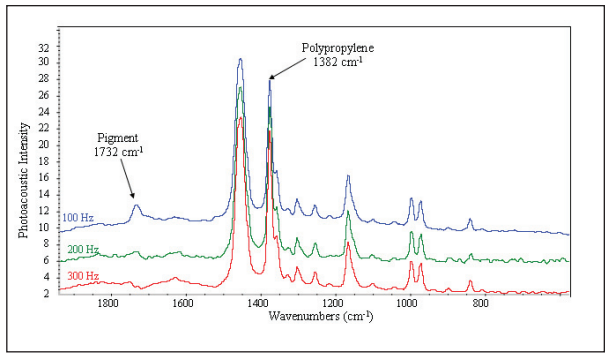

Figure 2: PA Magnitude spectra of food packaging laminate at four phase modulation frequencies. Strongest, clear features from individual layers are denoted.

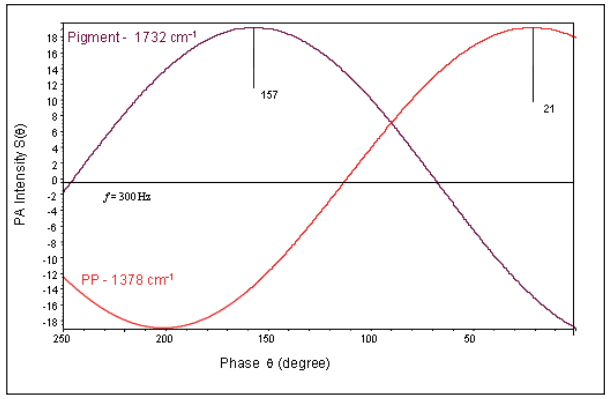

Figure 3: Plot of S(θ) vs. θ for the food packaging laminate indicating the relative phase position of the polypropylene (1378 cm^{-1}) and pigment (1732 cm^{-1}) bands at 300 Hz PM.

The thickness of 21.0 ± 0.5 μm calculated from the PAS measurements corresponds extremely well with the optical measurement of 22 mm observed for a sectioned sample under a microscope (Figure 1). At ΦM 100 Hz, the probing depth encompasses most of the pigment layer. PA signal saturation at lower modulation frequency tends to reduce the phase difference, and thus, the measured thickness as shown by the 100 Hz data.

ΦM Freq. Hz	Run#	1378 cm^{-1} PP Band Deg.	1732 cm^{-1} Pigment Deg.	ΔΦ Deg.	ΔΦ Rad	μ μm	PP Thickness μm		
100	1	9	80	71	1.24	15.8	19.5		
	2	10	84	74	1.29	15.8	20.4		
	3	10	86	76	1.33	15.8	20.9	*Ave*	20.4
	4	11	87	76	1.33	15.8	20.9	*STD*	0.6
200	1	30	141	111	1.94	11.1	21.6		
	2	30	138	108	1.88	11.1	21.0		
	3	32	133	101	1.76	11.1	19.6	*Ave*	21.1
	4	32	147	115	2.00	11.1	22.4	*STD*	1.1
300	1	21	157	136	2.37	9.10	21.6		
	2	21	155	134	2.34	9.10	21.3	*Ave*	21.5
	3	21	158	137	2.39	9.10	21.8	*STD*	0.2
						Ave	21.0		
						STD	0.5		

Table 1: Phase difference data and PP layer thickness calculations from the food packaging laminate representing multiple measurements at four phase modulation frequencies. Thermal diffusivity, $\alpha = 0.78 \times 10^{-3}$ cm^2/s was used for polypropylene.[8]

2. Coating on Elastomer

This sample consisted of a highly filled elastomer product with a very thin, delicate coating material. Previously, the only method to determine the coating thickness available to the manufacturer was gravimetric analysis of a solvent wash from a known area of the sample. The elastomer substrate is opaque and has a stippled surface making it difficult to work with by traditional spectroscopic methods. ATR spectra of the coated sample and the substrate collected with a Thermo Scientific OMNI-Sampler accessory (single-bounce, Ge crystal, depth of penetration ≈0.6 µm) are shown in Figure 5. The fact that the substrate features are clearly present in the top spectrum of the coated sample demonstrates that the coating is somewhat less than 0.5 µm thick.

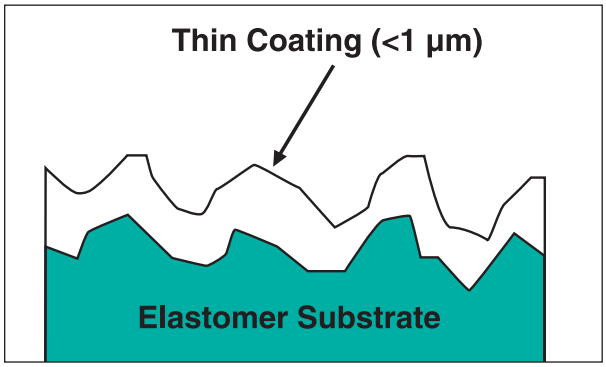

Figure 4: Highly filled elastomer with sub-micron thick coating.

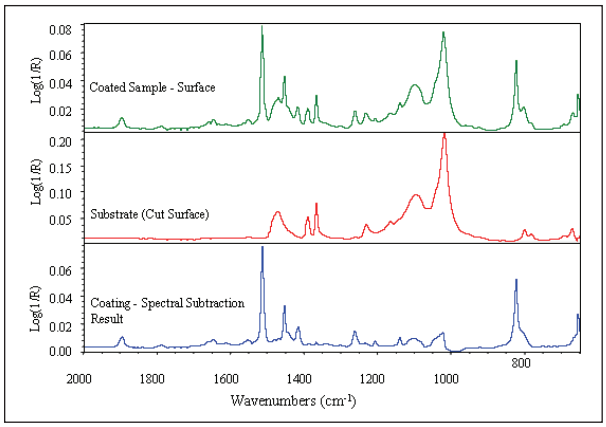

Figure 5: Ge ATR (D_p ≈ 0.6 µm) spectra of coated sample, substrate, and the spectral subtraction result yielding a "pure" coating spectrum.

Initial S²ΦM PAS experiments suggested that 500 Hz ΦM frequency was the optimum condition for the analysis, yielding the best signal-to-noise and an appropriate probing depth for the coating measurement. Figure 6 is a plot of the magnitude and phase spectra from the coated sample showing the slight phase difference between the characteristic coating and substrate bands. Replicate S²ΦM PAS measurements were made on four individual pieces of the sample. The phase difference measurements and the subsequent coating thickness calculations are listed in Table 2. The thermal diffusivity of the proprietary coating material was determined by the manufacturer.

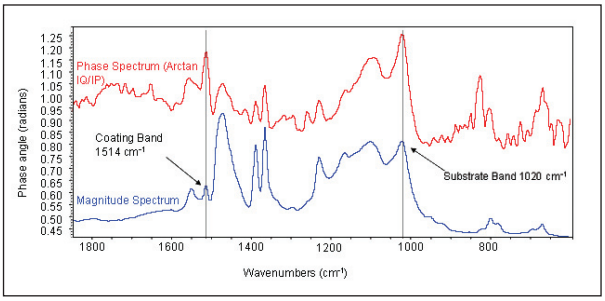

Figure 6: Magnitude and Phase spectrum of the coated elastomer sample collected at 500 Hz phase modulation frequency. The characteristic bands from the coating and the substrate are noted.

Piece#	Run#	1514 cm⁻¹ Coating Rad.	1020 cm⁻¹ Substrate Rad.	ΔΦ Rad.	µ µm	Coating Thickness µm		
1	1	1.257	1.276	0.019	10.88	**0.21**		
	2	1.237	1.251	0.014	10.88	**0.15**		
	3	1.200	1.222	0.022	10.88	**0.24**	Ave	**0.19**
	4	1.264	1.279	0.015	10.88	**0.16**	STD	**0.04**
2	1	1.174	1.203	0.029	10.88	**0.31**		
	2	1.166	1.177	0.011	10.88	**0.12**	Ave	**0.23**
	3	1.212	1.236	0.024	10.88	**0.26**	STD	**0.10**
3	1	1.184	1.207	0.023	10.88	**0.25**		
	2	1.247	1.265	0.018	10.88	**0.19**	Ave	**0.25**
	3	1.220	1.249	0.029	10.88	**0.31**	STD	**0.06**
4	1	1.218	1.244	0.026	10.88	**0.28**		
	2	1.249	1.292	0.043	10.88	**0.47**	Ave	**0.35**
	3	1.233	1.261	0.028	10.88	**0.30**	STD	**0.10**
						Ave 0.25		
						STD 0.09		

Table 2: Phase difference data and coating layer thickness calculations from the coated elasotomer sample representing multiple measurements at 500 Hz phase modulation frequency. Thermal diffusivity, $\alpha = 1.86 \times 10^{-3}$ cm²/s for the coating.[9]

While there was no direct method to check the result, the average thickness measurement corresponded well with the expectations of the manufacturer based on the previous gravimetric analysis. The variation from piece to piece and, to some extent, the scatter of the individual measurements was expected, as it was presumed that the coating thickness is not entirely consistent due to the uneven surface of the elastomer substrate.

Conclusions

This work demonstrates that the simplified phase difference model applied to S²ΦM PAS data is an effective, nondestructive method for the determination of coating layer thickness. While the technique works for relatively thick layers (greater than 10 mm), it is extremely beneficial for sub-micron layers which are difficult or impossible to measure by other means. In this work, only the top layer thickness was measured, but the technique offers the possibility to analyze subsurface layers as well. Future work should explore the application of other sophisticated models proposed previously[7] to the thickness measurement of multiple layers in complex laminates.

References

1. R.A. Shick, J.L. Koenig, and H. Ishida, *Appl. Spectrosc.* **50**, 1082 (1996).
2. F.M Mirabella, "Attenuated Total Reflection Spectroscopy," in *Modern Techniques in Applied Molecular Spectroscopy*, F.M. Mirabella, Ed. (Wiley Scientific, New York, 1998), Chap. 4, pp. 127-184.
3. N.J. Everall, *Appl. Spectrosc.* **54**, 773 (2000).
4. A. Rsencwaig and A. Gersho, *J. Appl. Phys.* **47**, 64 (1976).
5. J.F. McClelland, S.J. Bajic, R.W. Jones, and L.M. Seaverson, "Photoacoustic Spectroscopy," in *Modern Techniques in Applied Molecular Spectroscopy*, F.M. Mirabella, Ed. (Wiley Scientific, New York, 1998), Chap. 6, pp. 221-265.
6. Advanced FT-IR Spectroscopy, Thermo Fisher Scientific, Madison, WI (2003).
7. E. Y. Jiang, R.A. Palmer, and J.L. Chao, *J. Appl. Phys.* **78**, 460 (1995).
8. Y. S. Touloukian, R. W. Powell, C. Y. Ho and M. C. Nicolaou, "Thermal Diffusivity," Vol. 10, (IFI/Plenum, New York 1973), p. 593-619.
9. *Proprietary data supplied by material manufacturer*.

In addition to these offices, Thermo Fisher Scientific maintains a network of representative organizations throughout the world.

Africa
+43 1 333 5034 127
Australia
+61 2 8844 9500
Austria
+43 1 333 50340
Belgium
+32 2 482 30 30
Canada
+1 800 530 8447
China
+86 10 8419 3588
Denmark
+45 70 23 62 60
Europe-Other
+43 1 333 5034 127
France
+33 1 60 92 48 00
Germany
+49 6103 408 1014
India
+91 22 6742 9434
Italy
+39 02 950 591
Japan
+81 45 453 9100
Latin America
+1 608 276 5659
Middle East
+43 1 333 5034 127
Netherlands
+31 76 579 55 55
South Africa
+27 11 570 1840
Spain
+34 914 845 965
Sweden/Norway/ Finland
+46 8 556 468 00
Switzerland
+41 61 48784 00
UK
+44 1442 233555
USA
+1 800 532 4752

www.thermo.com

Thermo Electron Scientific Instruments LLC, Madison, WI USA is ISO Certified.

AN50811_E 05/08M